Proc. 28th Int. Conf. Coastal Eng. (ICCE 2002), pp. 1341-1352, ASCE, Cardiff.

BREAKING WAVE CHARACTERISTICS FOR THE LOADING OF A SLENDER PILE

- Large-Scale Model Investigations -

Kai Irschik[1], Uwe Sparboom[2], and Hocine Oumeraci[3]

Abstract: Large-scale model tests were carried out in the Large Wave Channel (GWK) with a slender cylindrical pile located at the end of a 1:10 slope. The test cylinder was subject to both regular and irregular waves. The paper deals with (i) the evaluation of the breaker characteristics at the breaking point for the test conditions, (ii) the comparison of the results with published data from small-scale experiments and (iii) the measured vertical distribution of horizontal particle velocities under a breaking wave. Additionally a new method of separating the measured force history into a slowly varying quasi-static and a dynamic part is presented by using the EMD (Empirical Mode Decomposition) for the analysis of breaking wave attack.

INTRODUCTION

The loading on a vertical slender pile is commonly calculated with the Morison equation. The total wave force F on the pile is described as a sum of a drag component F_D and an inertia component F_M as follows:

$$\begin{aligned} F &= F_D + F_M \\ &= \int \frac{1}{2} \cdot \rho \cdot D \cdot C_D \cdot u \cdot |u| \, dy + \int \rho \cdot C_M \cdot \frac{\pi \cdot D^2}{4} \cdot \dot{u} \, dy \end{aligned} \qquad (1)$$

where F_D, F_M = drag and inertia force; ρ = density of the water; D = diameter of the pile; C_D, C_M = force coefficients and u, $\dot{u}$ = horizontal particle velocity and acceleration.

1 Dipl.-Ing., Research Engr., FORSCHUNGSZENTRUM KÜSTE / „Coastal Research Centre“, Merkurstr. 11, D-30419 Hannover, Germany; irschik@fzk.uni-hannover.de.
2 Dr.-Ing., Senior Research Engr., FORSCHUNGSZENTRUM KÜSTE.
3 Prof. Dr.-Ing., Managing Director, FORSCHUNGSZENTRUM KÜSTE.

The force coefficients C_D and C_M are estimated experimentally. Considering a nonbreaking wave a wide range of values were determined for various flow conditions, e.g. see CERC (1984), Sparboom (1987), Sumer and Fredsøe (1997). Moreover the wave kinematics were addressed in many different laboratory and field investigations (see overview by Gudmestad (1993) for irregular waves). Figure 1a). shows an example for regular waves. For progressive, periodic waves a wave theory can be used to estimate the particle kinematics. In Figure 1a). the vertical distribution of the horizontal particle velocity is calculated by cnoidal theory (Fenton 1990) up to the mean water level followed by a linear decrease up to the water surface as proposed by Chakrabarti (1980).

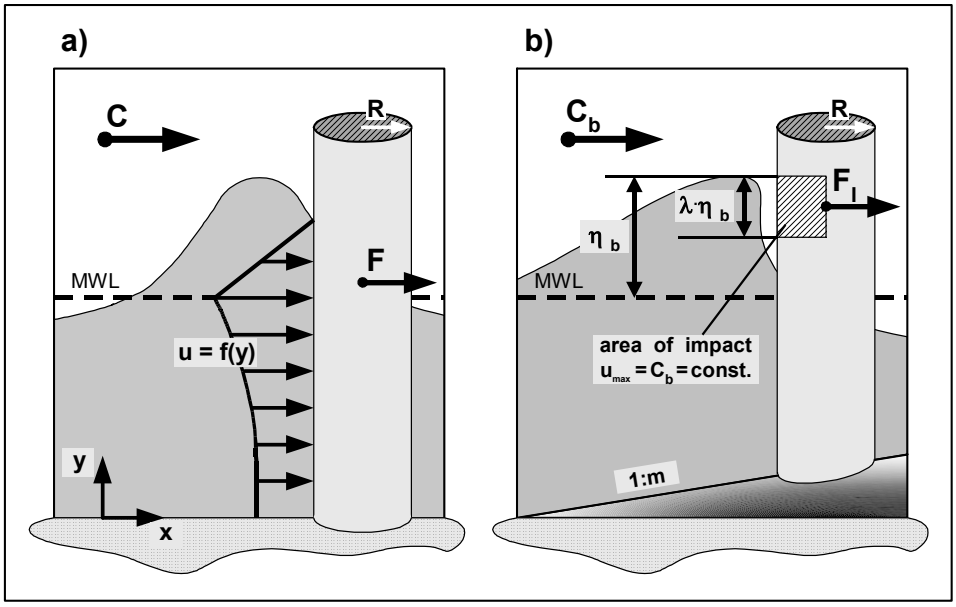

Fig. 1. a) Non-breaking wave and horizontal particle velocity distribution and b) impact area for a plunging breaker

Under breaking wave attack an additional force of short duration due to the impact of the vertical breaker front and the breaker tongue has to be taken into account (Figure 1b). Any attempt of applying Eq. 1 to this impact wave conditions must fail (Chaplin et al. 1992). The description of the total breaking wave force has therefore to be expanded by an additional impact force term F_I:

$$F = F_D + F_M + F_I \tag{2}$$

with:

$$F_I = \rho \cdot R \cdot C_b^{\,2} \cdot C_S \cdot \lambda \cdot \eta_b \tag{3}$$

where F_I = impact force; ρ = density of the water; R = radius of the pile; C_b = wave celerity at breaking point; C_S = slamming factor; λ = curling factor; η_b = maximum water surface elevation at breaking point (see Figure 1b).

The total breaking wave force on a slender pile (Eq. 2) is described by superposition of a slowly varying load, the quasi-static force represented by the MORISON equation, and a dynamic impact force. The formulation of the impact force (Eq. 3) is based on the assumption that the horizontal, two dimensional impact line force does not vary for different levels, i.e. the vertical distribution of the impact force remains constant over the height of the area of impact (Fig. 1b). The total impact force is obtained by introducing the curling factor λ, i.e. the height of the impact area is related to the maximum surface elevation at the breaking point η_b (see Figure 1b and Eq. 3). The value of the curling factor depends on the breaker type (Wiegel 1982, Wienke 2001).

The impact force depends not only on the breaker type, but also on the distance of the breaking point from the front of the cylinder (Tanimoto et al. 1986). Chan et al. (1995) and Wienke et al. (2000) have recognized five different loading cases by visual classification. Based on Eq. 3, Wienke (2001) developed a three-dimensional force model to estimate the maximum impact force on a slender pile analysing large-scale model tests with very steep breaking waves over a horizontal flume bottom.

For the design of near-shore pile structures (shallow water conditions) under breaking wave attack the probability of breaker occurrence and the corresponding breaking wave height H_b which depends on the water depth d_b and the beach inclination m must be known. Calculating the maximum impact according to Eq. 3 and the approach proposed by Wienke (2001) the values of the wave celerity C_b and the maximum surface elevation η_b at the breaking point are needed. Values of these wave parameters are presented below and compared with results from small-scale tests with different slope inclinations.

EXPERIMENTAL SET-UP

The tests were carried out in the Large Wave Channel (GWK) of the Coastal Research Centre in Hannover (LxWxD: 309 x 5 x 7 m). An 1:10 foreshore and an 1:17.5 slope at the end of the flume was heaped up with sand. The position of the test cylinder was at the very beginning of the berm as shown in Figure 2. The 1:10 slope was covered with an asphalt layer to ensure a stable surface. In the test series the water depth varied between 3.80 and 4.25 m,. The water depth in the berm area varied between 1.50 and 1.95 m. An overview of the wave gauges used in the study is given in Figure 2. 4 wave gauges were installed to measure the incident wave far in front of the slope, 12 gauges were distributed over the foreshore and four behind the smooth test cylinder made of steel. The test pile is 5 m long and has a diameter of 0.7 m (Figure 3). The structure was mounted on a steel beam 2.30 m above the flume bottom. At the top of the flume the pile was fixed at a traverse structure. Both bearings (top and bottom) were instrumented by strain gauges to measure horizontal wave forces. The total horizontal wave force is then calculated as the sum of the forces measured in the bearings. In the vertical frontline of the cylinder 16 pressure transducers were installed

in a distance of 0.2 m to each other. Additionally, 4 wave gauges were fixed at the test pile (Figure 3).

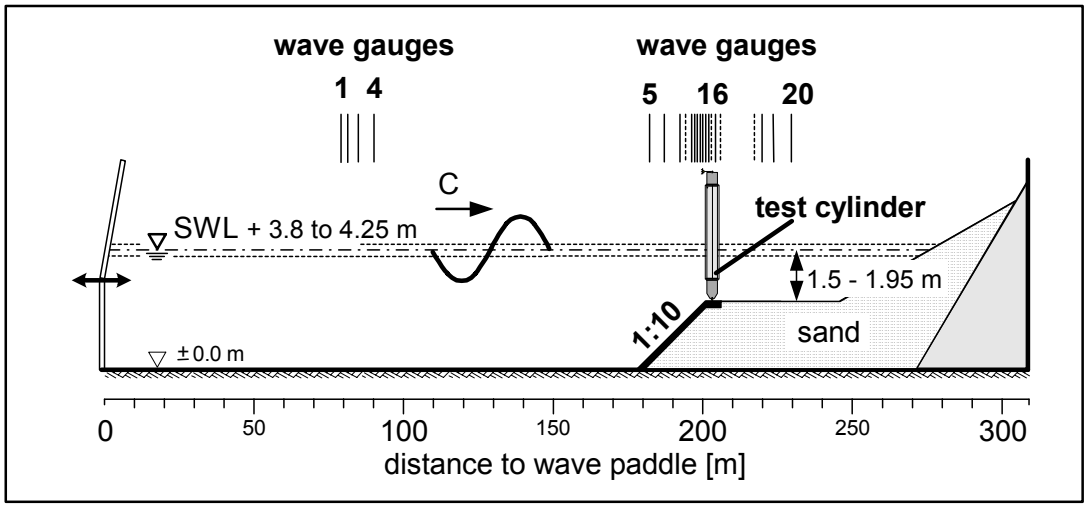

Fig. 2. Experimental set-up in the Large Wave Channel (GWK)

The horizontal components of the particle velocity were measured at different elevations. In the region from the berm bottom to the still water level 3-D acoustic doppler current meters (ADV) with a range up to ±7.5 m/s were used. Between SWL and the wave crest velocity measurements were conducted with 4 micropropellers. All probes were fixed on the wall at a location corresponding to the frontline of the test pile.

All data were recorded synchronously with a sampling rate of 200 Hz. This relatively low sampling rate was selected, because the spatial resolution of the pressure cells does not allow to obtain accurately the impact force, even for sampling rates in the order of 10 kHz. In fact, Wienke (2001) showed that the integration of the measured impact pressures to obtain the impact force is not justified in the area of impact. With the force transducers in the bearings the response of the pile is recorded. Therefore for the analysis of the impact force by using the force measurements the natural frequency of the test pile has to be taken into account ($\omega_E \approx 18$ Hz) and the sampling rate has been selected according to the pile response.

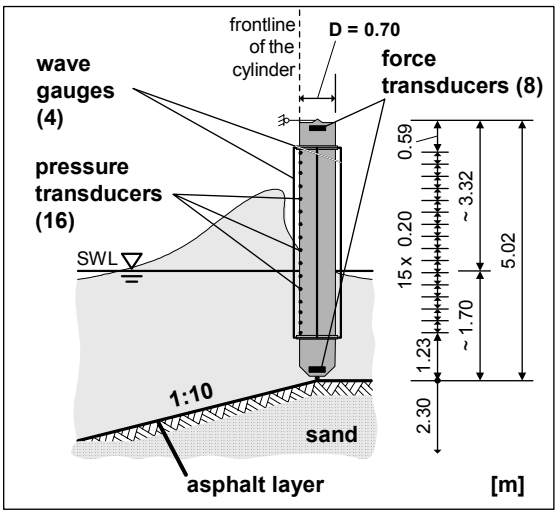

Fig. 3. Detail of the test cylinder

The wave parameters of regular wave tests reported in this paper are summarized in Table 1. The "deep water" wave steepness S_0 is calculated with the incident wave parameters H_0, L_0. The test runs generating plunging breakers are investigated predominantly in this paper.

Table 1. Wave parameters for the tests used in this paper

No. of runs	Water depth in the far field	Water depth at the pile	Wave Height H	Wave Period T	Deep Water Wave Steepness S_0
[-]	[m]	[m]	[m]	[s]	[-]
45	3.80-4.25	1.5-1.95	1.15-1.60	4.0-9.0	0.01-0.07

BREAKING WAVE CHARACTERISTICS

The breaking wave characteristics are determined for single waves of a test run, which are estimated with the zerodown-crossing method. In Figure 4 the breaking wave height H_b is related to the water depth d_b and plotted as a function of the relative breaking depth d_b/gT^2. The circles represent data recorded in the GWK. The grey filled, larger circle is one of these points as well. The error band is shown for this data point under the assumption, that the wave height H_b was underestimated ±2,5% and the breaking point lies ±0.5 m beside the first one. The difference between the squares shows the sensitivity of the single data points with regard to small uncertanties in the determination

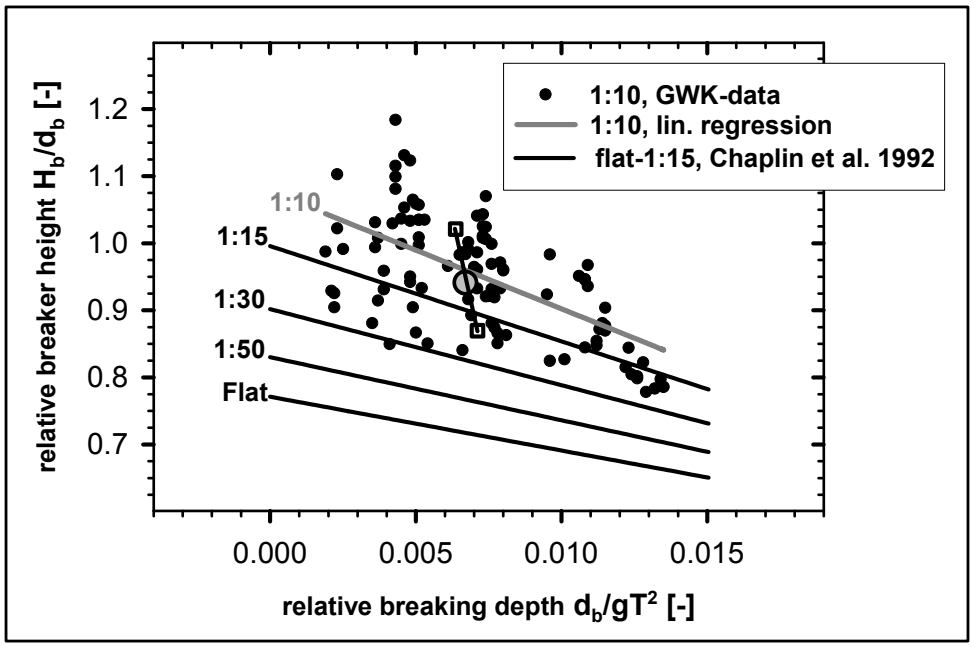

Fig. 4. Relative breaker height vs. relative breaking depth (comparison to the mean curves for other slope inclinations)

of the wave parameters and the breaking incident. Nevertheless, the comparison of the grey plotted mean curve of the H_b/d_b ratio to the mean curves presented by Chaplin et al. (1992) for different slope inclinations fits good, even if the range of the scatter is very high. The expected dependency of the breaker height on the slope inclination and the wave period is confirmed in Figure 4.

The relative wave celerity $C_b/g\,T$ and the relative surface elevtion $\eta_b/g\,T^2$ at the breaking point are evaluated from the records of the water surface elevation and can be seen in Figure 5. They are in good agreement with the mean curves of Chaplin et al. (1992). Both parameters are independent of the slope inclination. Scale effects cannot be observed from these results.

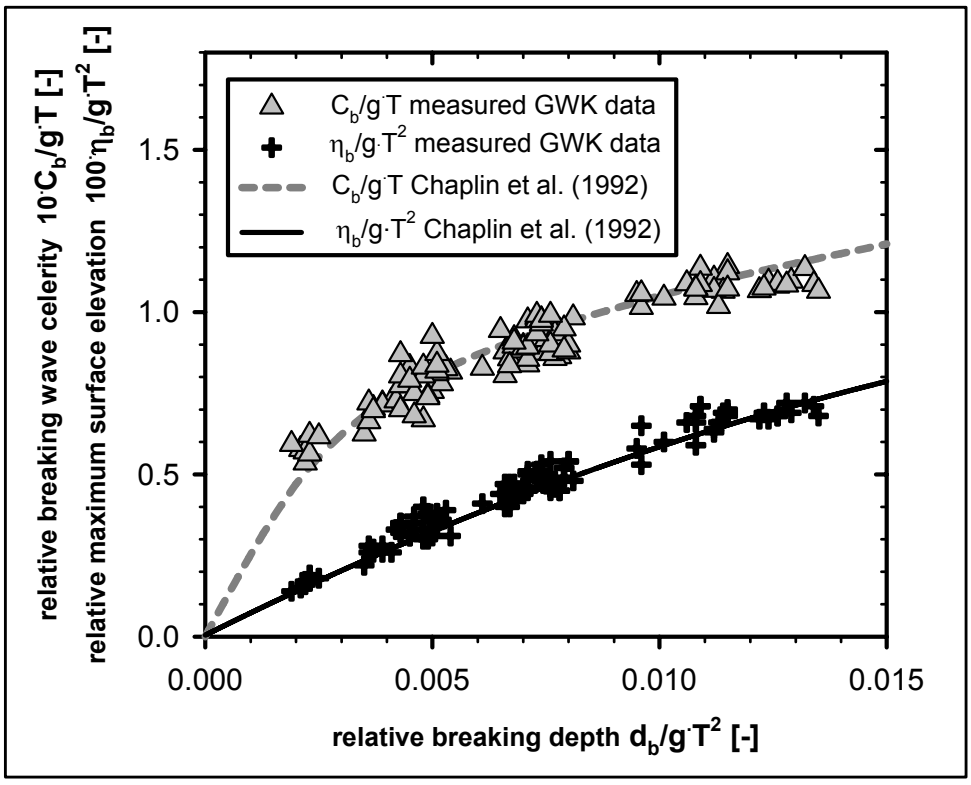

Fig. 5. Relative breaking wave celerity and relative maximum surface elevation vs. relative breaking depth

Figure 6 shows the maximum horizontal component of the particle velocity measured at different levels and scaled to a breaking depth of d_b = 1 m. The 4 lower circles and triangles up to the still water level are obtained from ADV-current meters, the upper two are measuered with micropropellers. The original still water level at incident breaking was 1.82 and 1.95 m. The vertical distribution up to the free surface shows the typical high increase of the velocity in the upper region of the plunging breaker. The GWK-data are also in good agreement with LDA-measurements of breaking waves published

by Griffiths et al. (1992). The velocities could be measured closer to the free water surface, thus allowing to confirm the assumption that the maximum horizontal particle velocity at the crest of a plunging breaker equals the wave celerity. The filled circle and triangle in Figure 6 symbolize the wave celerity estimated from the water surface elevation measurements. The elevation of these points represents the highest surface elevation of the breaking waves.

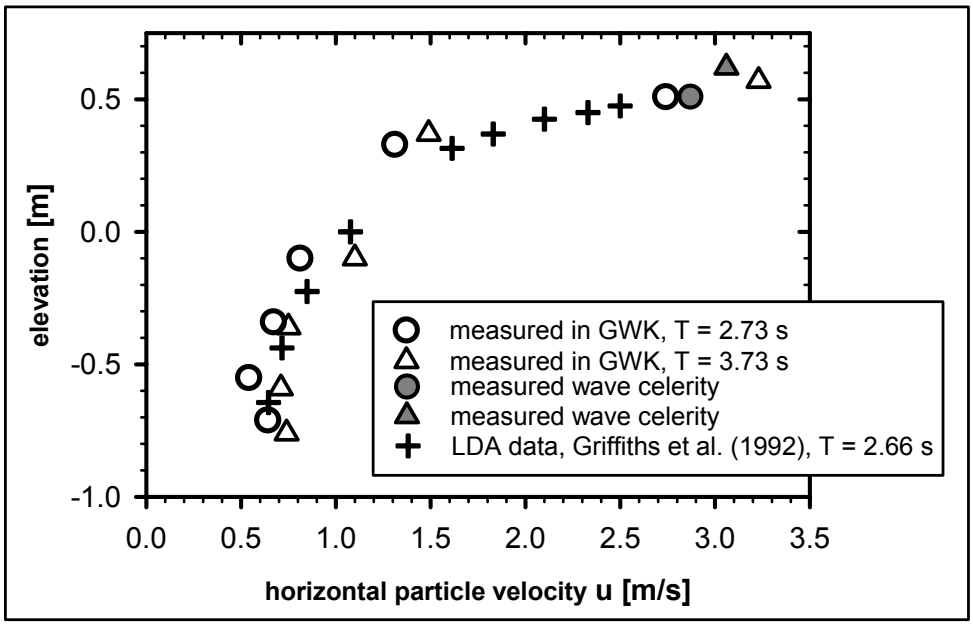

Fig. 6. Horizontal components of the particle velocity under the wave crest at the breaking point

PILE LOADING

According to Wienke et al. (2000) visual analysis of the tests is important for the identification of the loading cases, for the comparison of measurements and theoretical predictions. It is expected that Wienke´s theoretical approach will fit best for loading case 3 associated with the highest impact attack.

Loading cases (LC)

The distance of the breaking point to the front line of the pile is used to describe five loading cases. Visual analysis of the loading cases is made by estimating the breaking point and observing the wave front with the splash activity hitting the cylinder. In Table 2 the distance of the breaking point to the cylinder front decreases from loading case 1 to 4. For loading case 1 the wave breaking occurs far in front of the cylinder. Then the distance between the breaking point and cylinder front reduces, whereas in loading case 4 the wave breaks immediately at the cylinder and in case 5 there is no breaking in front of the pile. The distinction of the loading cases is made, since (i) the

Table 2. Classification of loading cases after Wienke et al. (2000)

	Description after Wienke et al. (2000)	**Principle sketch**	**Foto shot**
Load Case 1	• wave breaking far in front of the pile • broken wave • double peak: first peak due to breaker tongue; second one due to wave front	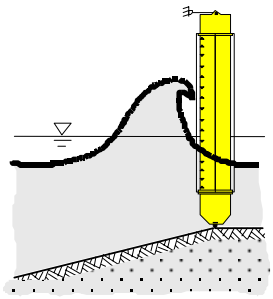	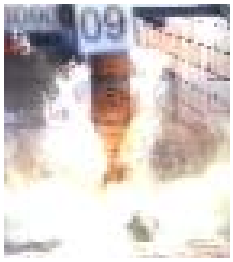
Load Case 2	• wave breaking in front of the pile • breaking wave • splash up- and downward • single and double peaks • overestimation of impact force due to assumption of simultaneous impact over the height	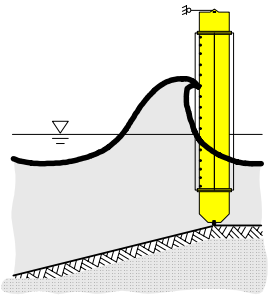	
Load Case 3	• wave breaking immediately in front of the pile • breaking wave • radial splash • single peak • assumption of simultaneous impact over the height is best fulfilled	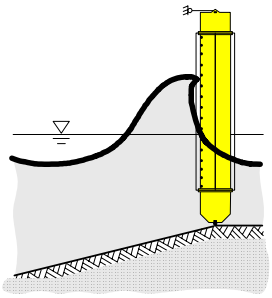	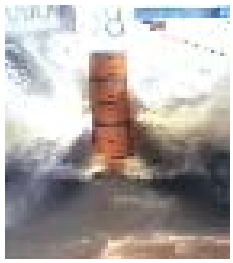
Load Case 4	• wave breaking at the pile • partial breaking wave • splash upward • single peak • force overestimation due to underestimation of impact duration	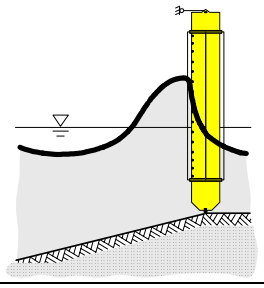	
Load Case 5	• no wave breaking at the pile • waves have considerably lower steepnesses than breaking waves	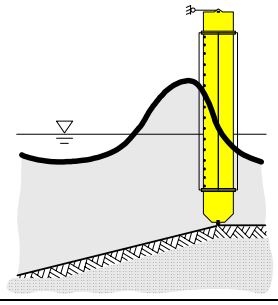	

impact varies in a high range between the loading cases and (ii) the response of the test pile is measured.

The estimation of the impact with the 3-D model of Wienke (2001) involves the assumption that the impact takes place over the whole height ($\lambda \cdot \eta_b$) of the impact area. The assumption is best fulfilled in loading case 3, since the breaker tongue and the wave front hit the cylinder nearly at the same time. This leads to the highest forces and accuracy in the analysis of the impact as a single peak. In loading case 2 the tongue hits the pile shortly before the wave front. In this case the time history of the force measurement shows double peaks or single peaks and turning points. The calculated impact will be overestimatred due to the mentioned assumption. Loading case 1 symbolizes the broken waves and in loading case 4 the impact is significantly lower than in loading case 3.

Empirical Mode Decomposition (EMD)

The theoretical description of the total breaking wave force is made by means of two independent approaches. The Morison equation to describe the quasi-static force and the 3-D impact model of Wienke (2001) to estimate the maximum dynamic force similar to loading case 3. Therefore a reliable separation of the quasi-static and dynamic part of the measured total force (Figure 7) is very important.

The separation of the recorded force measurements is often performed in frequency domain using e.g. a low pass filter. The drawback of this method consists in the choice of the cut-off frequency, which defines the frequency regions of the two force components. Using the EMD (Huang et al. 1999) this problem is avoided. The separation is carried out in time domain. The EMD is developed to transfer nonlinear, non-stationary processes into Instrinsic Mode Functions (IMF). The requirements of the IMF´s are that the mean value of the upper and lower envelope must be zero and that the number of extrema and zero-crossings must be equal or differ at most by one. Applying the EMD to the time history of the measured total force of Figure 7 (sum of the measured force in the bearings) the force is separated into six IMF´s and a residue part (Figure 8). The IMF 1 shows the high frequency part of the force and the frequencies getting lower up to the residue, the longest period. To complete the separation of the force, the high frequency IMF´s (1-4) are assigned to the dynamic component and the short frequency IMF´s (5+6) and

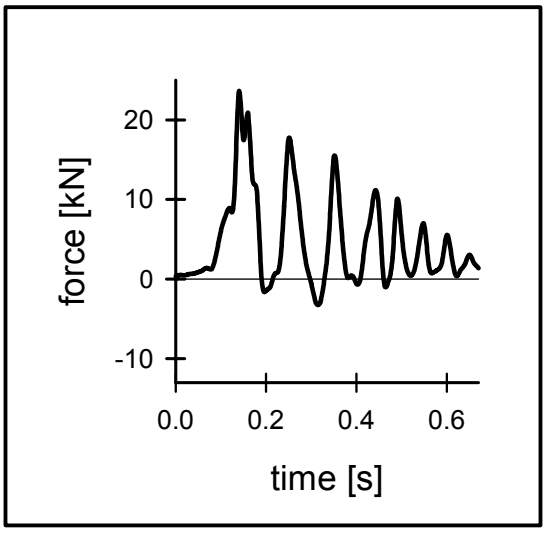

Fig. 7. Time history of the total measured force

the residue are summed to the quasi-static component. The result is depicted in Figure 9.

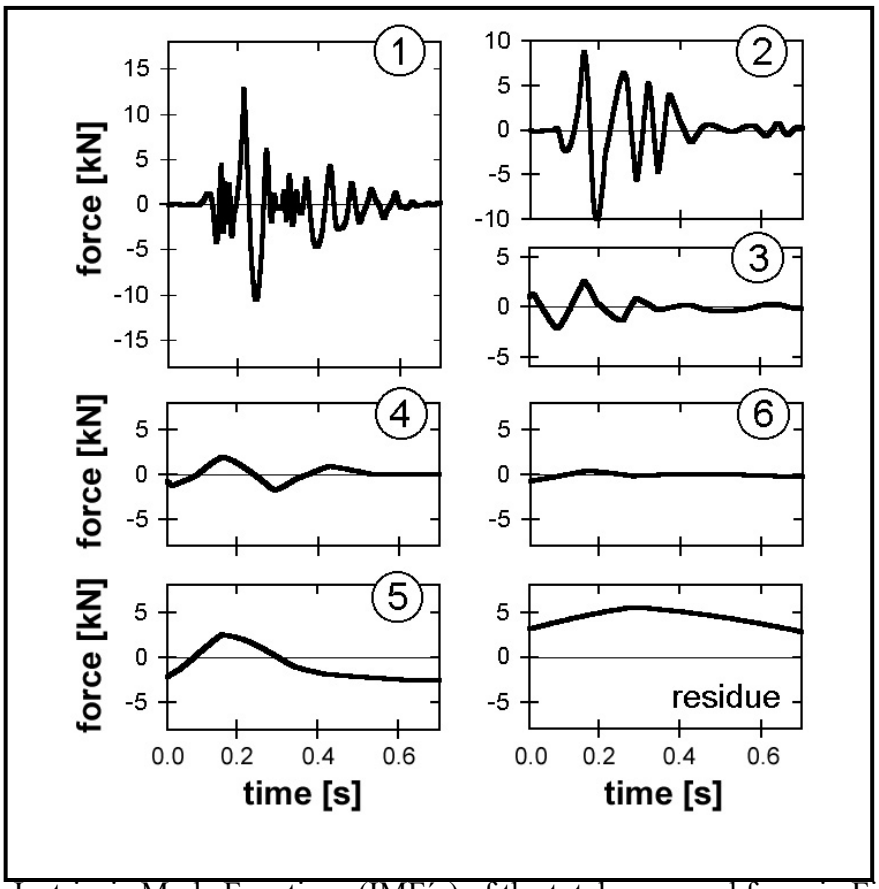

Fig. 8. Instrinsic Mode Functions (IMF´s) of the total measured force in Figure 7

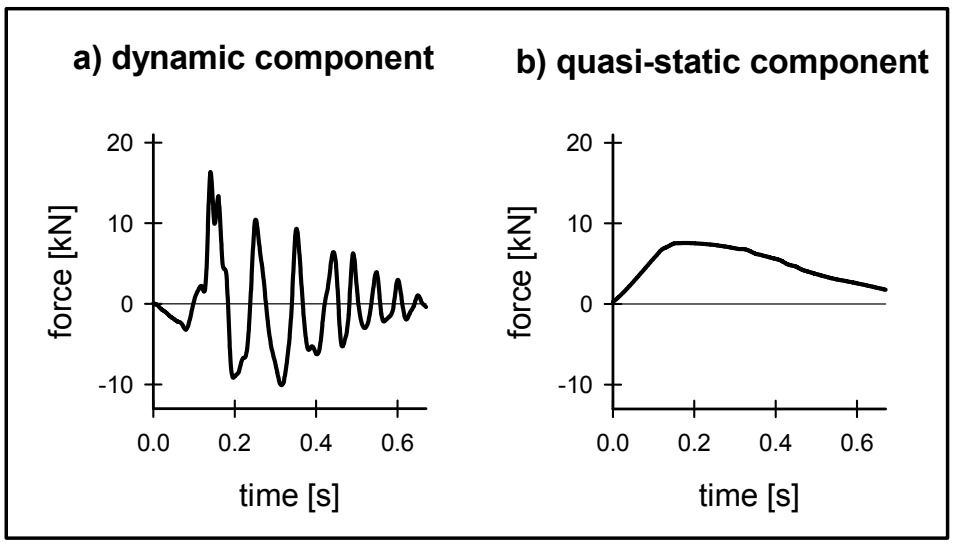

Fig. 9. a) Time history of the dynamic and b) quasi-static force estimated by using the EMD

The separated oscillations on the left represents the dynamic force (Figure 9a.). The plot on the right is the quasi-static force, which represents the loading case when no impact force is acting. The advantage of the EMD method is that the basis of the decomposition is directly derived from the measured data. This method can be applied to data of all loading cases.

CONCLUDING REMARKS

Large-scale model tests were carried out to measure the total wave force on a slender pile and the breaking wave kinematics synchronously. The breaking wave parameters H_b, C_b and η_b are estimated and the results of Chaplin et al. (1992) are enlarged due to the present study up to beach inclinations of 1:10. The measured horizontal component of the particle velocity is in good agreement with results of small-scale measurements by LDA. The assumption of the equality of the wave celerity and the maximum horizontal component of the particle velocity at breaking is confirmed.

The breaking wave force measurements are subdivided into five loading cases. It shows the dependence of the breaking wave force on the distance of the breaking point from the front of the pile. If the wave breaks immediately in front of the pile the maximum wave force occurs and the splash due to the hitting breaker develops radially.

The separation of the measured total force is performed by using the Empirical Mode Decomposition (EMD). This method is appropriate for the separation of the load into a slowly varying quasi-static and a dynamic part. The EMD can be applied to all force time histories with high accuracy irrespective of the loading case.

Further analysis of the force measurements is focussed on the theoretical evaluation of the two parts of the wave force and on the prediction of the maximum breaking wave load on slender piles under shallow water conditions.

ACKNOWLEDGEMENTS

The DEUTSCHE FORSCHUNGSGEMEINSCHAFT (DFG) supporting this basic research project “Belastung von zylindrischen Strukturen durch brechende und teilbrechende Wellen” (OU 1/4-2) is gratefully acknowledged by the authors.

REFERENCES

CERC 1984. *Shore Protection Manual*. Coastal Engrg. Res. Centre, U.S. Army Corps of Eng., Vicksburg, Mississippi.

Chakrabarti, S.K. 1980. Impact of analytical, model and field sutdies on the design of offshore structures. *Proceedings of the International Symposium on Ocean Engineeering, Ship Handling*, SSPA.

Chan, E.-S., Cheong, H.-F. and Tan, B.-C. 1995. Laboratory study of plunging wave impact on a vertical cylinder. *Coastal Engineering*, 25: 87-107.

Chaplin, J.R., Greated, C.A., Flintham, T.P. and Skyner, D.J. 1992. Breaking wave forces on a vertical cylinder. *Department of Energy Report*, OTH 90-324, 38 p.

Fenton, J.D. 1990. Nonlinear wave theories. In: Le Méhauté, B. and Hanes D.M. (eds.): *The Sea*, 9: 3-25.

Griffiths, M.W., Easson, W.J. and Greated, C.A. 1992. Measured internal kinematics for shoaling waves with theoretical comparisons. *Journal of Waterway, Port, Coastal and Ocean Engineering*, 118(3), 280-298.

Gudmestad, O.T. 1993. Measured and predicted deep water wave kinematics in regular and irregular seas. *Marine Structures*, 6: 1-73.

Huang, N:E., Zheng, S. and Long, S.R. 1999. A new view of nonlinear water waves: The Hilbert Spectrum. *Annual Review of Fluid Mechanics*, 31: 417-457.

Sparboom, U. 1987. Real wave-loads on small cylindrical bodies. *Proceedings of the 2nd International Conference on Coastal and Port Engineering in Developing Countries ´87*, COPEDEC.

Sumer, B.M. and Fredsøe, J. 1997. Hydrodynamics around cylindrical structures. *Advanced Series on Coastal Engineering*, 12, 530 p.

Tanimoto, K., Takahashi, S., Kaneko, T. and Shiota, K. 1986. Impulsive breaking wave forces on an inclined pile exerted by random waves. *Proceedings of the 20th International Conference on Coastal Engineering ´86*, ASCE, 2288-2302.

Wiegel, R.L. 1982. Forces induced by breakers on piles. *Proceedings of the 18th International Conference on Coastal Engineering ´82*, ASCE, 1699-1715.

Wienke, J., Sparboom, U. and Oumeraci, H. 2000. Breaking wave impact on a slender cylinder. *Proceedings of the 27th International Conference on Coastal Engineering ´00*, ASCE, 1787-1798.

Wienke, J. 2001. *Druckschlagbelastung auf schlanke zylindrische Bauwerke durch brechende Wellen – Theoretische und großmaßstäbliche Untersuchungen*. Dr. Thesis, Tech. University Carolo-Wilhelmina of Braunschweig, Leichtweiss-Institute, 102 p (in German).